

05,09

## Relaxation of electron spins of nitrogen centers in structural channels of beryl crystal

© R.B. Zaripov<sup>1</sup>, I.T. Khairutdinov<sup>1,¶</sup>, R.I. Mashkovtsev<sup>2</sup>

<sup>1</sup>Zavoisky Physical-Technical Institute FRC Kazan Scientific Center RAS, Kazan, Russia

<sup>2</sup>Sobolev Institute of Geology and Mineralogy, Siberian Branch Russian Academy of Sciences, Novosibirsk, Russia

¶ E-mail: semak-olic@mail.ru

Received April 2, 2025

Revised May 23, 2025

Accepted May 25, 2025

The electron spin-spin and spin-lattice relaxation times of two types of nitrogen centers localized in structural channels of a beryl crystal are measured. The measurements are performed using the electron spin echo method at different orientations of the crystalline sample relative to a constant magnetic field and in a wide temperature range. It is shown that the spin-spin relaxation time of both centers is practically the same and does not depend on orientation. In the temperature range from 300 to 5 K, it varies non-monotonically within the limits from 5100 to 2400 nanoseconds. The spin-lattice relaxation time varies from 0.15 milliseconds to 2 milliseconds in the temperature range from 300 to 5 K.

**Keywords:** relaxation, beryl crystal, electron spin echo, quantum memory, coherence.

DOI: 10.61011/PSS.2025.05.61493.65-25

### 1. Introduction

An electron spin is a good candidate for the role of a quantum bit (qubit). One of the concepts of building a quantum computer on electron spins is building chains of electron spins placed into insulating matrices. The role of the insulating matrix is to reduce the negative effect of the environment at the coherence of electron states. A good container in this case is a carbon frame of fullerene [1–4]. Qubits in this case were electron-nucleus spin systems of nitrogen and phosphorus atoms enclosed in fullerene [5]. However, creation of such a chain is accompanied with significant technical problems. Several years ago it was reported that beryl crystal may also be used as a matrix for qubits. It is related to the fact that it contains structural channels in the form of a chain made of cavities with size of around 5 Å, separated with convergences of 2.8 Å diameter [6]. These cavities may enclose atoms of hydrogen, nitrogen and silver. It is known that atomic hydrogen is stabilized in structural channels of beryl at room temperature [7]. Nitrogen and silver atoms maintain their paramagnetic properties up to the temperature of around 250 °C [8]. Structural channels of beryl crystal investigated in the paper contain nitrogen atoms in two magnetic-nonequivalent positions. This manifests in the spectra of stationary electron paramagnetic resonance (EPR) in the form of a superposition of triplets of isotropic hyperfine structure from nitrogen nuclei <sup>14</sup>N with two different constants of fine structure.

One of the important characteristics of using the spin system as elements of quantum informatics are the decoher-

ence processes. Phase relaxation time  $T_f$  is specific time, when the spin qubit remains coherent. This time must be rather long compared to the time of manipulations with the spins. Currently the requirements to the real scaled systems are much stricter: modern methods of quantum correction of errors require around 10 000 operations to be performed within the decoherence time [9]. The spin-lattice relaxation time  $T_1$  is a time interval, when the qubit must be measured at the end of the quantum computation. Time  $T_f$  may be considered as the specific time to store the quantum information, and time  $T_1$  may be considered as the specific time to store the classic information.

### 2. Spectrum of beryl crystal electron spin echo signals

This paper measured the relaxation times at nitrogen atoms in structural channels of beryl using electron spin echo (ESE) spectroscopy. Beryl has hexagonal crystal system, space group  $P6/mcc(D_{6h}^2)$ . Synthetic crystals of beryl were grown at 600 °C and pressure of 1 kbar from solution NH<sub>4</sub>Cl, and then exposed to annealing.

Measurements were carried out using spectrometer Elexsys E580 (Bruker) in X frequency range (9.8 GHz). The spectrometer is equipped with a commercial dielectric resonant cavity ER4118MD5W1 (Bruker), placed in a cryostat CF935 (Oxford), a programmable uniaxial goniometer ER218PG1 (angle variation range 0–360°, positional accuracy is equal to 0.5°) (Bruker). The measurements were made in the wide temperature interval 5–300 K. Temperature was monitored with a temperature controller

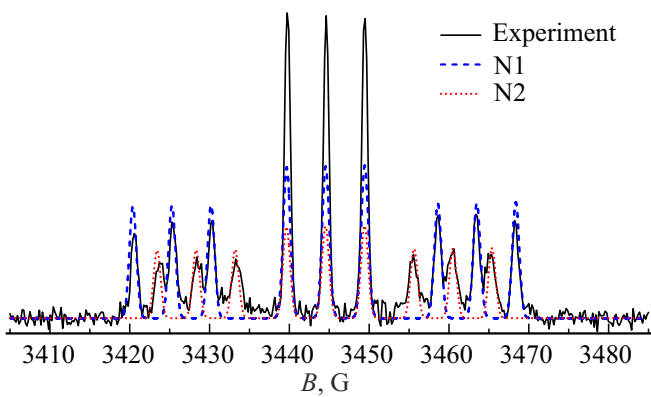


**Figure 1.** The spectrum of ESE signals from nitrogen centers N1 and N2 at 300 K with structural axis  $c$  of beryl equal to  $30^\circ$  relative to permanent magnetic field. Dashed line — modeling of spectrum N1, dotted line — of spectrum from center N2.

ITC503 (Oxford). To rotate the crystal in the magnetic field, an adjusted bar was used with the ability to rotate in two planes. A crystal holder is a fluoroplastic cylinder, where a specimen is placed. The outer diameter of the cylinder is 4.4 mm, and the height — 2.8 mm. The cylinder with the specimen is placed at the bottom end of the rod and is installed inside the dielectric resonant cavity. On the opposite side of the rod a rotation system with a graduated arc was installed. Rotation from the upper part to the lower part was transferred with the help of a silk thread. The additional rotation system makes it possible to rotate this cylinder with the specimen by  $360^\circ$  around axis  $Z$  or  $Y$  of the laboratory coordinate system. The crystal structural axis  $c$  was produced using a 2D goniometer and corresponded to 0 degrees in the experimental data. Spectra of ESE signals and phase relaxation time were recorded using the primary echo protocol with duration of  $\pi/2$ -pulse equal to 8 ns [10]. The time of spin-lattice relaxation was measured by protocol „inversion–recovery“ with duration of  $\pi/2$ -pulse 8 ns [10]. When building the spectrum of ESE signals and signal „inversion–recovery“ the integral intensity of the echo was applied. When the time of phase relaxation was measured, ESE signals were recorded for each pulse-to-pulse interval  $\tau$ . Then these signals were exposed to Fourier transform. The droop amplitude of each peak in the Fourier-spectrum depending on time  $\tau$  was modeled with exponential dependence.

Figure 1 shows the spectrum of ESE signals at room temperature with the magnetic field  $30^\circ$  orientation relative to the crystal structural axis  $c$ . The lines of triplets are observed from two non-interacting paramagnetic center of nitrogen N1 and N2 (see the red and blue lines in Figure 1) with the intensity ratio of approximately 2 : 1. Note that the atoms in the traps are observed in the states close to that of a free atom with a spin equal to  $S = 3/2$  [11,12].

Both paramagnetic centers N1 and N2 have the symmetry that is axial relative to the structural axis and the same value of hyperfine interaction (HFI)  $A = 4.9$  G. For each center

there are three transitions of the fine structure corresponding to spin  $3/2$ . The EPR spectrum may be described with a spin Hamiltonian:

$$\hat{H} = g\beta BS_z + D[S_z^2 - 1/3S(S+1)] + AS_zI_z, \quad (1)$$

where  $S_z$  and  $I_z$  — operators of projections at axis  $z$  of the electron spin and nitrogen nucleus spin, accordingly,  $D$  — constant of fine structure,  $A$  — HFI value of electron with nitrogen nucleus  $^{14}\text{N}$ ,  $g$  —  $g$ -factor,  $\beta$  — Bohr magneton,  $B$  — permanent magnetic field value. The modeling results match the data in paper [8], where the following values of parameters were identified:  $g = 2.0021$ ,  $A = 4.9$  G,  $D = 15.9$  G and 13.4 G for N1 and N2, accordingly.

It is not possible to effectively excite the entire spectrum with width of around 50 G in the experiment, since the amplitude of microwave pulses has the value of not more than 10 G. Therefore, the ESE measurements were made in individual areas of the spectrum by changing the carrier frequency of microwave pulses. Fourier transforms of the measured ESE from the certain areas of the spectrum were produced. These Fourier transforms quite well follow the shape of the spectrum areas, which is shown in Figure 2.

The echo signal amplitude decreases with the increase of the delay between the two microwave pulses  $\tau$  — first of all, due to the process of spin-spin relaxation with the characteristic time  $T_f$ . As a result, the amplitude of components in the Fourier transforms decreases, which enables to track the speed of relaxation in all spectrum components, simultaneously excited by the microwave pulses.

### 3. Times of electronic paramagnetic relaxation

Dependences of the spectrum component amplitudes on the orientation and time of delay between the microwave pulses made it possible to build a 2D dependence of spin-spin relaxation time distribution on angle  $\theta$  for centers N1 and N2 (Figure 3).

By analysis of the times of spin-spin relaxation  $T_f$  for all components in the wide range of angles one may conclude on their relatively weak spread by absolute value (see Figure 3). Values  $T_f$  are mostly within 4000–5400 ns at room temperature. Note that for canonic orientations the values of phase relaxation times are slightly higher than for interim orientations.

Measurements  $T_f$  were made in the same manner for the three central components, which do not depend on angle  $\theta$  (see the parallel lines in the center in Figure 3) in the wide temperature range from 5 to 300 K. From Figure 4,  $a$  you can see that the produced values  $T_f$  in this range are within 2400 - 5100 ns, and the produced temperature dependence is not monotonous.

Temperature dependence of longitudinal relaxation time is expected — time  $T_1$  increases sharply when temperature falls from 0.15  $\mu\text{s}$  (at 300 K) to 2 ms (at 5 K). Temperature

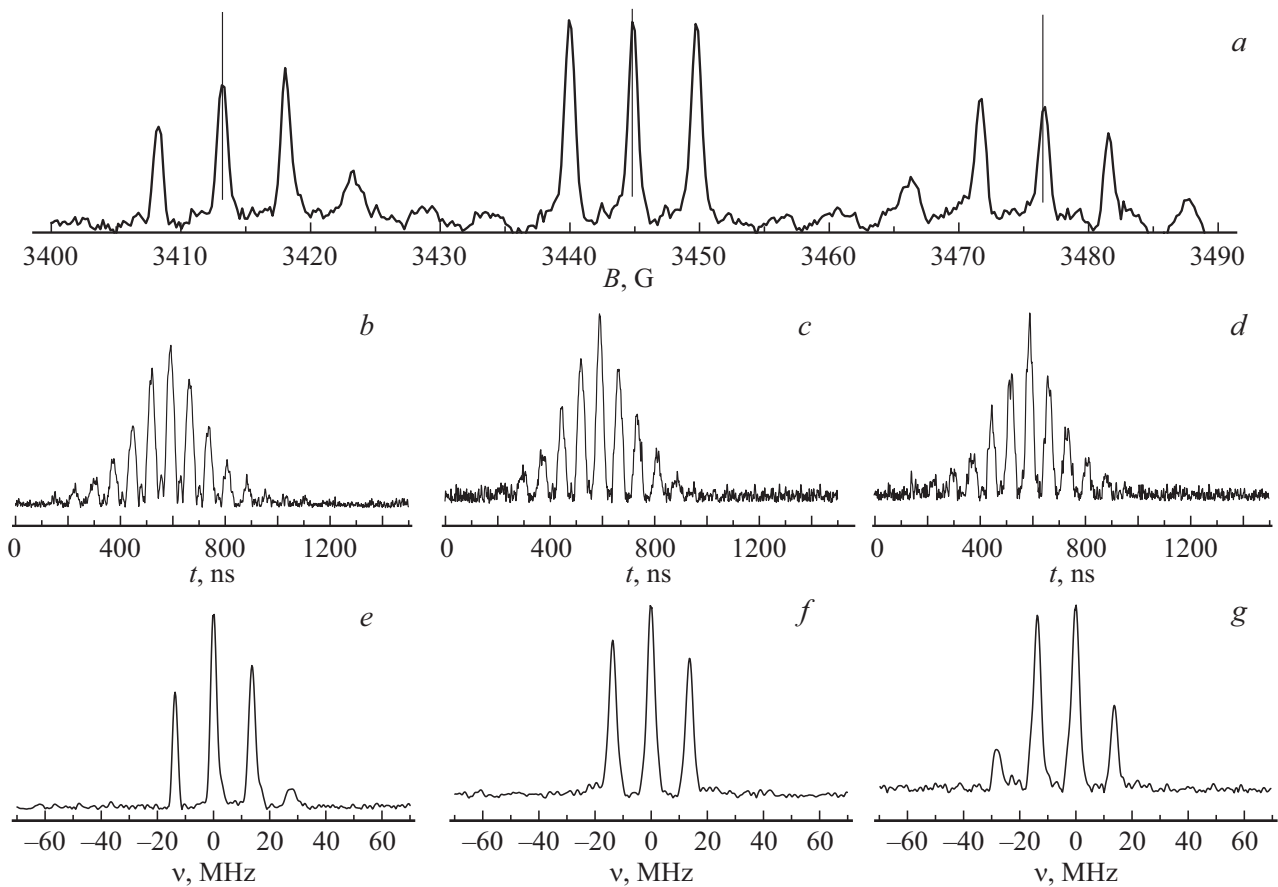


**Figure 2.** *a* — Spectrum of ESE signals of nitrogen centers N1 and N2 at 300 K with orientation of beryl structural axis at the angle  $0^\circ$  relative to permanent magnetic field; *b–d* — ESE signals at  $\tau = 320$  ns from the areas of the spectrum, the centers of which are shown by vertical lines in Figure 2, *a*; *e–g* — Fourier transforms of ESE signals shown in Figure 2, *b–d*.

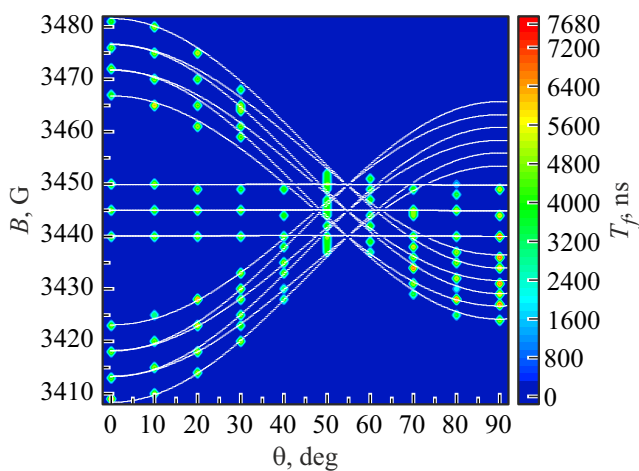


**Figure 3.** 2D dependence of spin-spin relaxation  $T_f$  time distribution on magnetic field value  $B$  and orientation ( $\theta$ ) of crystal in the magnetic field. Values of times  $T_f$  are shown in color according to the color palette on the right. White lines indicate the theoretical positions of resonance transitions for centers N1 and N2. The data are shown at room temperature. For technical reasons, the measurements of relaxation times in the area of magnetic fields 3455–3470 G and angles  $\theta$  from 70 to  $90^\circ$  were not made.

dependence of phase relaxation time  $T_f$  looks more interesting. From Figure 4 you can see that as temperature decreases from 300 to 20 K, the relaxation times first decrease, and then increase again. One of the options for the potential behavior is the effect of spectral diffusion [13]. Previously it was shown [14] that structural channels of beryl crystal contain no impurities. The most common impurities — molecules of water and ammonia ions [15]. Dipole-dipole interaction between the electron spins of paramagnetic centers and nuclear spins of these impurities may widen the EPR signal lines. The value of dipole-dipole interaction of  $\Delta$  proton with nitrogen atom has the value of around 0.4 G at distance 4 Å. This distance is an approximate size of the cavity in the structural channel. Such contribution is quite noticeable on the background of the line width of around 1 G. Dipole-dipole interaction with the ammonia nitrogen nucleus in this case is by one order less than with proton and it is negligible. The motion of the closest water molecules also changes of the value of hyperfine interaction with protons. This causes a random change in the value of resonance frequency of EPR in paramagnetic centers N1 and N2. Such motion is an effective mechanism for phase relaxation of ESE signal [16].

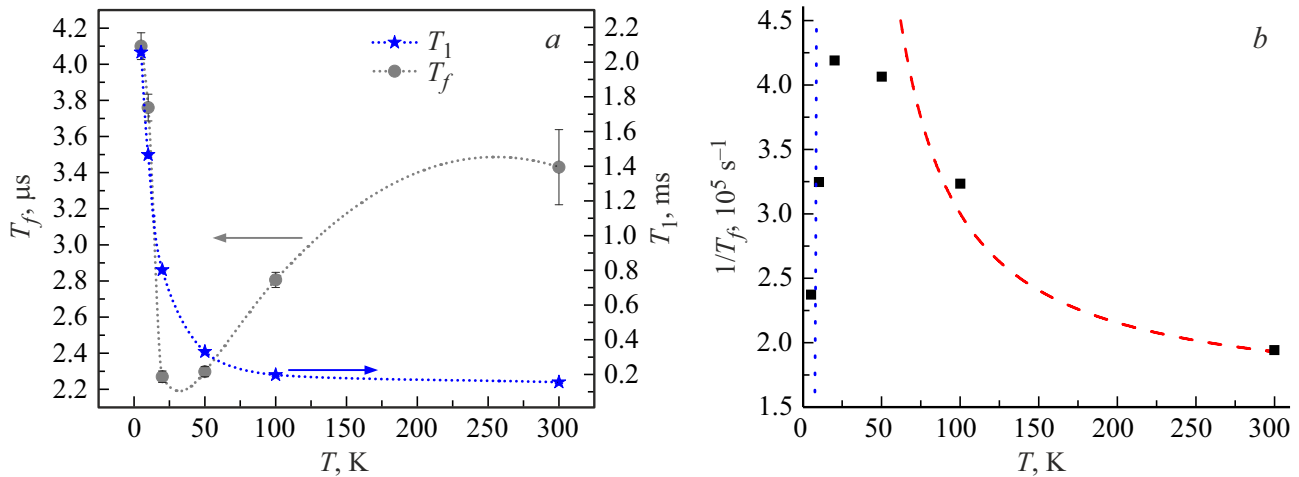


**Figure 4.** *a* — Integral dependence of time of phase  $T_f$  (grey circles) and spin-lattice  $T_1$  (blue stars) relaxation upon excitation of the central ( $B_0 = 3444$  G) component of the central triplet depending on temperature; *b* — Speed of relaxation of the central component depending on temperature (black squares). Dotted line — theoretical dependence of relaxation speed in approximation of slow motion. Dashed line — in approximation of fast motion. Crystal axis *c* is parallel to the direction of the magnetic field.

To assess the impact of nuclear spins at time behavior of echo signals, the ESE signal decay rate calculations were made in the approximations of fast and slow motion. The echo signal amplitude  $E(2\tau)$  in the case of fast motion, i. e. under the condition  $\tau_c^{-1} \gg \Delta$ , looks rather simple [13,17]

$$E(2\tau) \approx \exp[-2\tau(\Delta^2\tau_c/2)], \quad (2)$$

where  $\Delta^2\tau_c/2$  is the signal decay rate,  $\tau_c$  — correlation time,  $\Delta$  — value of interaction in frequency units. Echo signal amplitude  $E(2\tau)$  in case of slow motion, i. e. provided that  $\tau_c^{-1} \ll \Delta$  signal of electronic spin echo looks as follows

$$E(2\tau) \approx \exp[-2\tau/\tau_c], \quad (3)$$

where  $1/\tau_c$  is the signal decay rate. Figure 4, *b* shows the approximations of the experimental dependence of relaxation speed with two curves — for slow motion with speed of  $1/\tau_c$  and for fast motion with speed  $\Delta\tau_c^2/2$ . Temperature dependence of the correlation time  $\tau_c$  was applied as [18]

$$\frac{1}{\tau_c} = \frac{1}{\tau_{c0}} \exp[-B/(RT)], \quad (4)$$

where  $\tau_{c0}$  — time of correlation in high-temperature range,  $B$  — activation energy,  $R$  — universal gas constant. As a result of modeling, the following values of parameters were received:  $1/\tau_{c0} = 7 \cdot 10^9 \text{ s}^{-1}$ ,  $\Delta = 1.4 \cdot 10^6 \text{ s}^{-1}$ ,  $B = 550 \text{ cal/mol}$ . In such approximations the estimated curves of echo signal droop amplitude are qualitatively described as experimental.

## 4. Conclusion

For the first time the times of electron relaxation of paramagnetic centers of nitrogen in the beryl crystal

structural channel were measured. The time of spin-spin relaxation  $T_f$  at room temperature is within 4000–5400 ns. It is practically the same for paramagnetic centers N1 and N2 and hardly depends on the orientation of the structural axis relative to the permanent magnetic field. Temperature dependence of time  $T_f$  is not monotonous, reaching the maximum value of 2400 ns at 20 K. The time of spin-lattice relaxation changes practically using the exponential law, reaching the values of 0.15 ms at room temperature and 2 ms — at helium temperature.

Non-central lines of paramagnetic centers N1 and N2 are resolved well depending on the crystal orientation in the magnetic field, which makes it possible to target their spin states with microwave pulses. Besides, the system of paramagnetic centers has the spin-spin relaxation time that hardly varies with temperature and without anisotropic properties, which may be useful as the material for quantum memory.

## Funding

The study was supported by the grant of the Russian Science Foundation No. 22-72-10063, <https://rscf.ru/project/22-72-10063/>. All experiments were carried out at the collective spectrum and analytical Center of Physical and Chemical Research of Substances and Materials and Substances Structure, Properties and Composition, FRC Kazan Scientific Center RAS.

## Conflict of interest

The authors declare that they have no conflict of interest.

## References

- [1] W. Harneit. Phys. Rev. A **65**, 032322 (2002).
- [2] D. Pinto, D. Paone, B. Kern, T. Dierker, R. Wiczorek, A. Singha, D. Dasari, A. Finkler, W. Harneit, J. Wrachtrup, K. Kern. Nature Commun. **11**, 6405 (2020).
- [3] D. Suter, K. Lim. Phys. Rev. A **65**, 052309 (2002).
- [4] J. Twamley. Phys. Rev. A **67**, 052318 (2003).
- [5] A.A. Popov. Endohedral Fullerenes: Electron Transfer and Spin. Springer International (2017).
- [6] N.V. Belov, R.G. Matveeva. Tr. Instituta kristallografii AN SSSR **6**, 69 (1951).
- [7] V.F. Koryagin, B.N. Grechushnikov. FTT **7**, 8, 2496 (1965). (in Russian).
- [8] R.I. Mashkovtsev, V.G. Thomas. Appl. Magn. Reson. **28**, 401 (2005).
- [9] A.M. Steane. Phys. Rev. A **68**, 042322 (2003).
- [10] A. Schweiger, G. Jeschke. Principles of Pulse Electron Paramagnetic Resonance. Oxford University Press (2001).
- [11] A.L. Buchachenko, A.M. Vasserman. Stabilnye radikaly. Khimiya, M. (1973).
- [12] D. Dins, D. Vinyard. Radiation-induced defects in solid bodies. Inostr. Lit., M. (1960).
- [13] K.M. Salikhov, A.G. Semenov, Yu.D. Tsvetkov. Elektronnoe spinovoe ekho i ego primenenie. Nauka, Sibirskoe otdelenie, Novosibirsk (1976).
- [14] R.I. Mashkovtsev, V.P. Solntsev. Phys. Chem. Minerals **29**, 1, 65 (2002).
- [15] J.L. Zimmermann, G. Giuliani, A. Cheillett, C. Arboleda. Int. Geol. Rev. **39**, 425 (1997).
- [16] L.D. Kispert, M.K. Bowman, J.R. Norris, M.S. Brown. J. Chem. Phys. **76**, 26 (1982).
- [17] G.M. Zhidomirov, K.M. Salikhov. Zh. Eksp. Teor. Fiz. **56**, 1933 (1969).
- [18] R.G. Hayes, D.J. Steible, W.M. Tolles, J.W. Hunt. J. Chem. Phys. **53**, 4466 (1970).

*Translated by M. Verenikina*